

## Full Paper

**Design and Development of Novel 4-(4-(1*H*-Tetrazol-5-yl)-1*H*-pyrazol-1-yl)-6-morpholino-*N*-(4-nitrophenyl)-1,3,5-triazin-2-amine as Cardiotoxic Agent via Inhibition of PDE3**Zhi-Wei Mao<sup>1</sup>, Qiao-Ling Li<sup>2</sup>, Ping Wang<sup>1</sup>, Yang-Li Sun<sup>1</sup>, and Yu Liu<sup>1</sup><sup>1</sup> Department of Cardiovasology, Zhengzhou Central Hospital Affiliated to Zhengzhou University, Zhengzhou, Henan, P. R. China<sup>2</sup> Department of Kidney Rheumatology, The Fifth Affiliated Hospital of Zhengzhou University, Zhengzhou, Henan, P. R. China

The classical phosphodiesterase 3A (PDE3A) inhibitors provide relaxation of the vasculature system via increasing the cellular level of cyclic adenosine monophosphate (cAMP) and proved to be useful in the management of congestive heart failure. Consequently, the present paper deals with the development of novel pyrazole derivatives tethered with substituted 1,3,5-triazine derivatives in search for novel PDE3 inhibitors. The synthesis of designed inhibitors was realized in a multi-step reaction and the structures were ascertained with the help of various spectroscopic techniques. Subsequently, these analogs were tested for their inhibitory activities against PDE3 enzymes, where they exhibited considerable inhibition, revealing **9g** as the most promising inhibitor of the class. In a docking study, the morpholine fragment of compound **9g** was efficiently engulfed in the small pocket of the active site lined by Gly940 and Pro941. The substituted aromatic ring of the core scaffold was found to be positioned deep in the cavity bordered by Tyr829, Asn830, Leu850, Glu851, and Thr893. Moreover, it considerably improved the contractility of cardiac muscles without altering the heart beat frequency in experimental subjects.

**Keywords:** 1,3,5-Triazine / Docking / PDE3 inhibitor / Synthesis

Received: October 26, 2015; Revised: January 20, 2016; Accepted: January 26, 2016

DOI 10.1002/ardp.201500388



Additional supporting information may be found in the online version of this article at the publisher's web-site.

**Introduction**

The morbidity and mortality associated with cardiovascular diseases (CVDs) have put a selective pressure for their effective treatment and prevention. It is a rapidly increasing public health concern for both developed and developing nations. The severity of the disease has been easily understood by its widespread nature, which accounts for the loss of 17.5 million people in 2012, representing 31% of all global deaths [1–3].

Among the CVDs, failure of the heart or congestive heart failure (CHF) is regarded as a chronic manifestation which results in inadequate supply of the blood to meet the demand of various organs due to diminished cardiac function. It is a grave life-threatening situation, demonstrating the end-stage of an innumerable other cardiac anomalies without a remedial cure [4]. Concerning to this, novel and effective medication are needed urgently.

Against CHF, presently two lines of therapeutic interventions have been used, i.e., glycoside- and non-glycoside agents. The glycoside drugs are mainly based on digitalis and have been associated with serious side-effect, including acute arrhythmias along with a low therapeutic index [5].

**Correspondence:** Dr. Ping Wang, Department of Cardiovasology, Zhengzhou Central Hospital Affiliated to Zhengzhou University, No. 195 Tonbai Middle Road, Zhengzhou, Henan 450000, P. R. China.

**E-mail:** wangpingcr@hotmail.com**Fax:** +86-371-67690000

Zhi-Wei Mao and Qiao-Ling Li contributed equally to this work.

However, the drugs belonging to the category of non-glycoside agents do not have any significant extra-effects and are able to act as a cardiotoxic agent via selective inhibition of cyclic nucleotide phosphodiesterase (PDE) enzymes. It is deemed to be responsible for maintaining the endogenous level of cyclic adenosine monophosphate (cAMP) and cyclic guanosine monophosphate (cGMP), a second messenger. According to the physiological functions and substrate specificity, it was further sub-divided into 11 different families exerting numerous roles, viz., PDE1–11. Among the enzyme class, particularly PDE3 is considered to induce vascular contraction and its inhibition causes relaxation of the vasculature system via increasing the cellular level of cAMP. It was further sub-divided into PDE3A and PDE3B depending upon its occurrence, for instance, cardiac tissues and hepatocytes, respectively. Thus, its inhibition offers symptomatic relief in CHF [6, 7].

More recently, pyrazole-based compound has been reported to exhibit potent PDE3 inhibitory activity (Fig. 1) [8, 9]. The derivatives originating from 1,3,5-triazine are also behaving as potent medicinal agents, such as, antibacterial [10], antimalarial [11], anticancer [12], antifungal [13], antidiabetic [14], anti-CFTR [15], carbonic anhydrase inhibitors [16], anti-HIV [17], and others. Concerning to this, present paper deals with the development of novel pyrazole derivatives tethered with substituted 1,3,5-triazine derivatives in search of novel PDE3 inhibitor.

## Results and discussion

### Chemistry

The synthesis of target analogs was achieved in numerous consecutive steps as outlined in Scheme 1. Initially, the

commercially available 2,4,6-trichloro-1,3,5-triazine (**1**) was selected as starting template which later underwent nucleophilic reaction with morpholine in the presence of activating base to yield compound **2**. Whereas, various amines were selected depending upon the chemical nature to be substituted on above-synthesized compound to afford corresponding derivative **3**. Moreover, the remaining chloro of 1,3,5-triazine was easily replaced with hydrazine under reflux to furnish compound **4** in excellent yield. It was further allowed to react with malonaldehyde bis-(dimethyl acetal) which results in the cyclization of terminal hydrazine to pyrazole (**6**), a core scaffold; according to the method described by Finar and Godfrey. The synthesis of compound **7** was achieved under Duff's condition via selective formylation of compound **6**, while it was further allowed to react with hydroxylamine to afford compound **8**. The synthesis of target analogs was achieved via refluxing above synthesized compound with  $\text{NaN}_3$  using  $\text{AlCl}_3$  as a catalyst in DMF. The compounds were obtained in excellent yield and considerable purity as determined via various analytical techniques.

The FT-IR absorption bands of final compounds are shown in the experimental section. The N–H stretching frequency was observed at  $3431\text{--}3438\text{ cm}^{-1}$ . The strong band at  $1621\text{--}1649\text{ cm}^{-1}$  is attributed to the C=N stretching frequency. The Ar C–H group stretching frequency was observed at  $3052\text{--}3065\text{ cm}^{-1}$ . Moreover, the presence of Cl on the phenyl ring was observed at  $784\text{--}786\text{ cm}^{-1}$ . The (–N=N–) group of tetrazole was observed at  $1571\text{--}1589\text{ cm}^{-1}$ , whereas  $\text{OCH}_3$  group on the phenyl ring was observed at  $2924\text{--}2928\text{ cm}^{-1}$ .

The final compound showed another band at  $1156\text{--}1162\text{ cm}^{-1}$  which is attributed to primary C–F stretching frequency. Moreover, the presence of C=N group of tetrazole was confirmed at  $1621\text{--}1649\text{ cm}^{-1}$ . The  $^1\text{H NMR}$

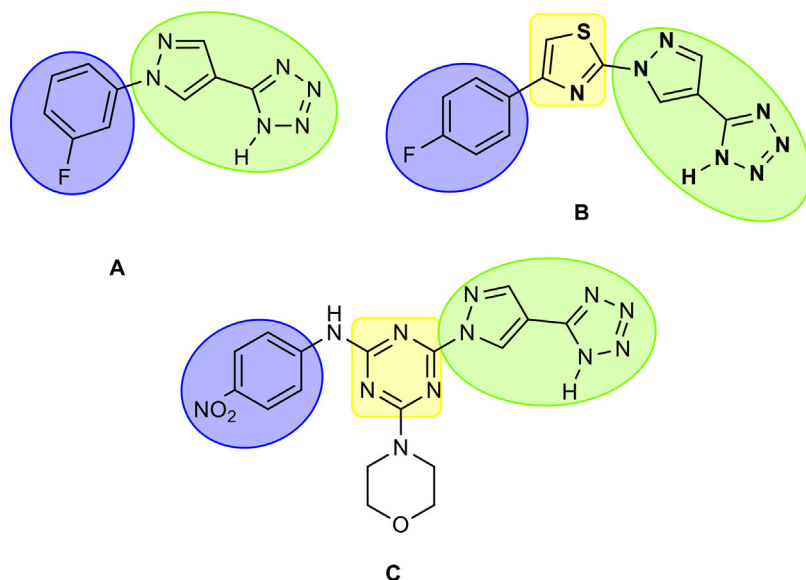
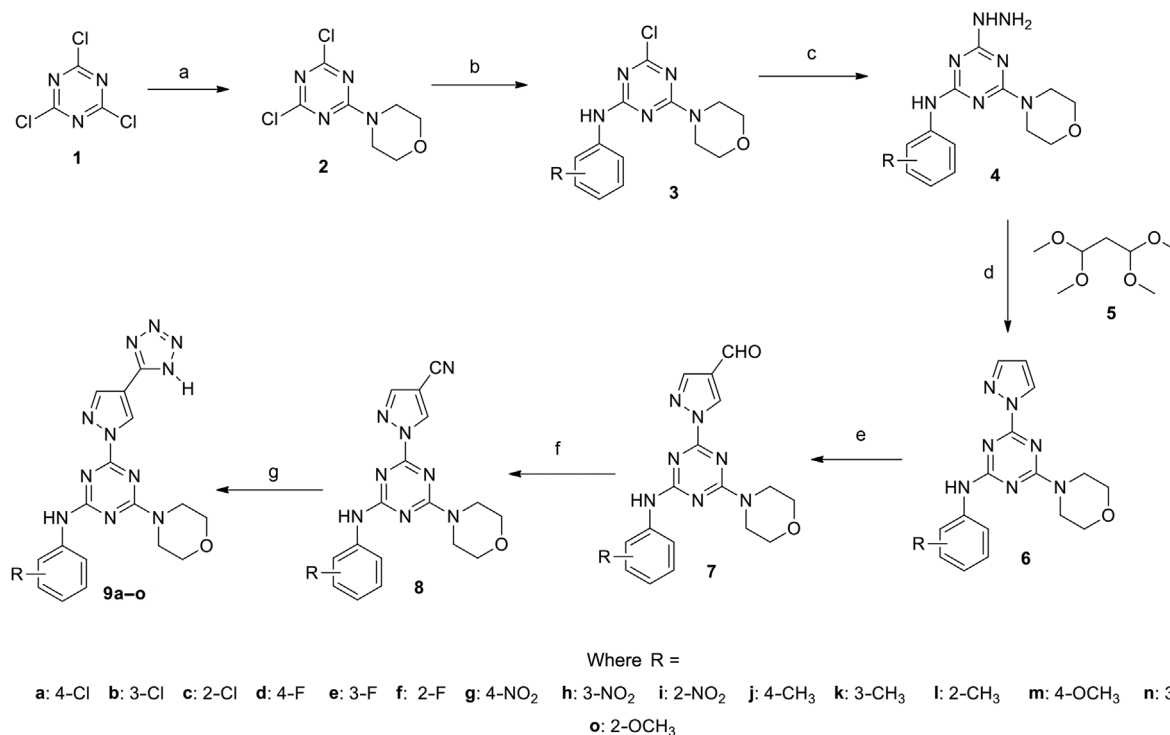


**Figure 1.** Structures of the various pyrazole-based analogs (A and B) and of the designed inhibitor (C) developed in the present study.



**Scheme 1.** Synthesis of the target compounds. Reagents and conditions: (a) aq. NaOH soln., 0–5°C, stirring; (b) aq. NaOH soln., 40–45°C; (c) KHCO<sub>3</sub>, reflux; (d) HCl, EtOH, reflux; (e) HMTA, CF<sub>3</sub>COOH, reflux; (f) NaI, NH<sub>2</sub>OH, DMF, reflux; (g) NaN<sub>3</sub>, DMF, AlCl<sub>3</sub>.

spectra showed at 8.02–6.18 ppm which is attributed to the resonance of Ar–H. The resonance of methyl proton was found as a singlet in the region 2.18–2.35 ppm, whereas another singlet corresponds to 3.82–3.84 ppm for proton of methoxy group. The resonance of pyrazole protons was found as a doublet in the region 8.84–8.84 ppm. Finally, all the structures of final compounds were recognized by mass and elemental analysis.

### Pharmacological activity

As presented in Table 1, various target derivatives were assessed for possible inhibition of PDE3 (types A and B) enzyme (see also the Supporting Information for the InChI codes). It has been found that entire set of target compounds exhibit considerable range of inhibition against both the variants of PDE3, e.g., PDE3A and PDE3B. Among the synthesized compounds, **9a** showed moderate inhibition of PDE3A (IC<sub>50</sub> = 9.10 ± 0.04 μM) and PDE3B (IC<sub>50</sub> = 13.43 ± 0.23 μM). While on varying the position of substituent, the inhibitory potency was reasonably reduced as found in the case of compounds **9b** and **9c** against both the variants of PDE3. The presence of fluoro on the flanked aromatic ring of the core scaffold showed considerable improvement in the inhibitory potency which suggests that *para*-substituted derivative (**9d**) was found more active than its isomeric counterparts, viz., **9e** and **9f**. The highest inhibitory potency

was disclosed by the compounds containing nitro as the substituent with prominent inhibition in the case of compound **9g** against PDE3A and PDE3B with IC<sub>50</sub> 0.33 ± 0.01 and 5.20 ± 0.09 μM, respectively. Whereas, its isomeric replacement leads to the marginal loss of the activity as evidenced by the inhibitory potency of compounds **9h** and **9i**. The activity was further diminished in the case of the rest of the compound having electron donating substituents, viz., –methyl (**9j–l**) and –methoxy (**9m–o**). It was surprising to note that compounds containing methyl as a substituent showed prominent reduction in activity against PDE3B than PDE3A in comparison to compounds having electron-withdrawing groups.

The structure–activity relationship study corroborated that the entire set of synthesized compounds showed a similar pattern of inhibition against PDE3A than PDE3B, with more prominent action against PDE3A. While in comparison to standard, only few compounds exhibit much prominent action than vesnarinone. Particularly, compounds containing nitro (**9g–i**) and fluoro (**9d–f**) along with **9a** were found to inhibit PDE3 enzymes more significantly than their congeners. Among the synthesized compounds, analogs containing electron-withdrawing group showed considerable activity compared to electron-donating compounds. Moreover, the position of substituent was also found critical for the generation of the bioactivity, for instance, a minor isomeric variation in core scaffold renders compound non-active or less

**Table 1.** Inhibitory activity of target compounds against PDE3.

Compound	IC <sub>50</sub> (μM)	
	PDE3A	PDE3B
9a	9.10 ± 0.04	13.43 ± 0.23
9b	12.32 ± 0.11	18.16 ± 0.12
9c	14.23 ± 0.12	19.03 ± 0.18
9d	4.43 ± 0.13	4.10 ± 0.04
9e	8.34 ± 0.15	6.22 ± 0.02
9f	7.45 ± 0.11	14.03 ± 0.16
9g	0.33 ± 0.01	5.20 ± 0.09
9h	1.23 ± 0.32	6.45 ± 0.14
9i	2.23 ± 0.05	12.32 ± 0.13
9j	18.22 ± 0.12	36.36 ± 0.11
9k	23.32 ± 0.23	45.19 ± 0.17
9l	28.45 ± 0.33	67.86 ± 0.20
9m	33.18 ± 0.17	ND
9n	42.64 ± 0.15	ND
9o	52.56 ± 0.22	ND
Vesnarinone	10.22 ± 0.21	15.45 ± 0.21

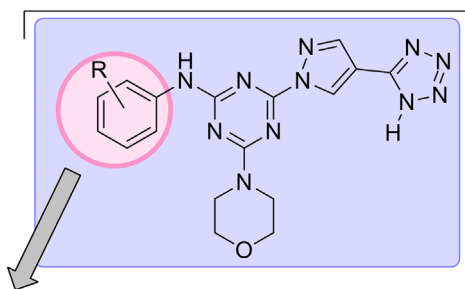
active. It has been further found that *para*-substituted derivative showed significant inhibitory activity than either of *ortho* and *meta* counterparts. The structure–activity relationship (SAR) of the target analogs has been clearly outlined in Fig. 2.

### In silico study of compound 9g

Docking study is considered as a powerful computational tool which can easily predict the preferred orientation of ligand into the protein of interest via many algorithmic approaches [18]. Thus, in the current study, protein model

### Effect on the Inhibitory Activity

#### PDE3A > PDE3B



#### Order of group

NO<sub>2</sub> > F > Cl > CH<sub>3</sub> > OCH<sub>3</sub>

#### Position of substituent

4 > 3 > 2

**Figure 2.** Structure–activity relationship of the target analogs for PDE3 inhibition.

of PDE3 was selected to perform the docking of compound **9g** to elaborate the key intermolecular interactions necessary for the inhibitory activity. As shown in Fig. 3, **9g** was efficiently accommodated inside the catalytic site of the PDE3 enzyme via making prolific interactions with the neighboring residues. It was found that the morpholine fragment was engulfed in the small-pocket lined by Gly940 and Pro941. Whereas, the substituted aromatic ring of core scaffold was found to be positioned deep in the cavity bordered by Tyr829, Asn830, Leu850, Glu851, Thr893, and Asp894 via formation of one H-bond with Asn830. Apart from it, **9g** revealed the formation of two non-covalent π–π stacking interaction with Phe991 via involvement of 1,3,5-triazine and pyrazole. The results of the docking study indicated that designed inhibitor was appreciably accommodated deep inside the catalytic site of protein and was thereby able to inhibit its catalytic function for inhibitory activity. To further find out the key structural fragment necessary for the activity, based on the docked orientation, a pharamcophore-based model was generated and is presented in Fig. 4. These computational results are found in accordance with the earlier studies and provide valid evidence for the efficient inhibitory activity of **9g** against PDE3A [9].

### Effect of compound 9g as inotropic and chronotropic activities

Encouraged by the excellent PDE3A inhibitory activity of compound **9g**, it is worthwhile to perform its possible effect on the force of contraction and the frequency rate of heart of experimental rat. This study is more imperative to perform because the PDE3A enzymes are highly expressed in cardiac tissues. Thus, the effect of **9g** on the above-discussed parameters was determined by the impulsively beating atria of rat. However, the endogenous catecholamine (CAs) release can interfere with the study, so the animal was pre-treated with reserpine to block the release of any CAs [19]. The study was performed in comparison to vesnarinone as a standard and the results are presented in Table 2. From the results, it was easily concluded that **9g** does not affect the frequency rate and is not able to induce any arrhythmias. It is noteworthy to mention that the effect of compound **9g** was considerably found lower than vesnarinone as standard. On the other hand, as assumed, it showed drastic improvement in contractility of cardiac muscles (79 ± 3) and even much better than standard (51 ± 1) at 100 μM.

### Conclusion

We have developed a novel series of hybrid pyrazole-1,3,5-triazine conjugates as potent inhibitors of PDE3 with more selective inhibition against the PDE3A over PDE3B. Moreover, these molecules proved to enhance the force of contraction rather than frequency of heart beat, which makes them as a prospective lead for future drug discovery. However, more

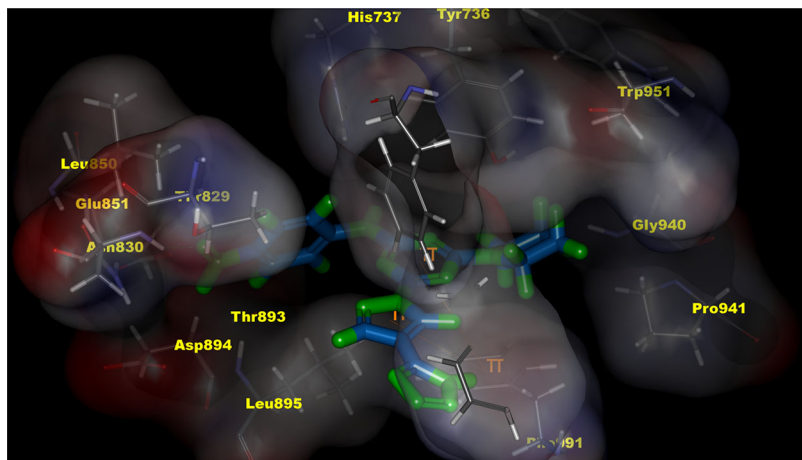


Figure 3. Docked orientation of compound **9g** in PDE3.

studies are needed to be performed for exact elucidation of its molecular mechanism.

## Experimental

### Chemistry

All chemicals were obtained from commercial suppliers and used directly without further purification unless specified. The

melting points of the synthesized derivatives were quantified in digital melting point apparatus and are uncorrected. TLC was used to analyze the completion of the reaction using silica gel-G coated Al-plates and were detected under UV (254 nm) and in chamber containing iodine vapor. Flash-1112 series elemental analyzer was used for determination of carbon, hydrogen, and nitrogen. IR spectra (KBr) were recorded on a PerkinElmer FT-IR. The  $^1\text{H}$  NMR and  $^{13}\text{C}$  NMR spectra were recorded on a Bruker Avance-500 NMR spectrometer and

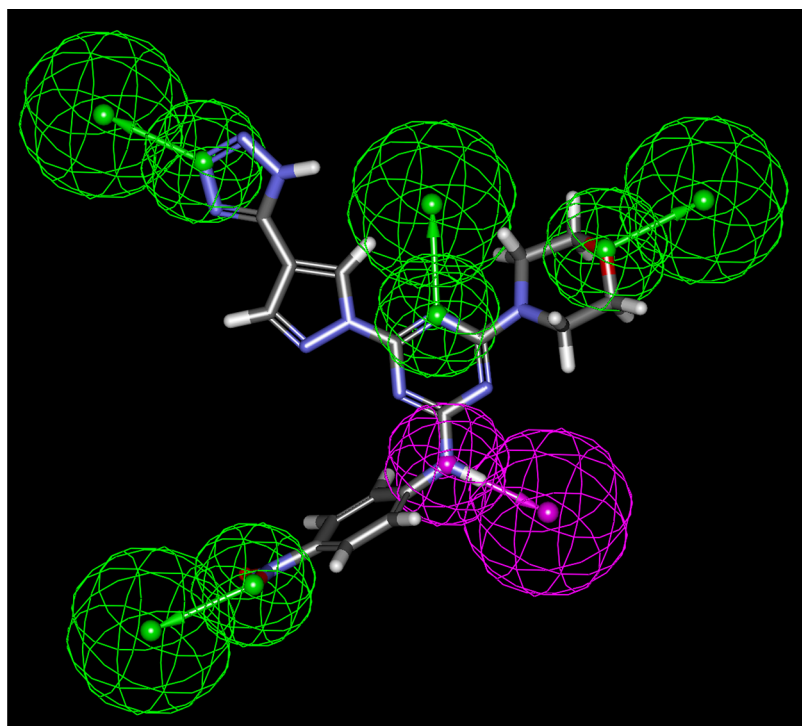


Figure 4. Structure-based pharmacophores model of **9g** for inhibition of PDE3.

**Table 2.** Pharmacological evaluation of compound 9g on the heart of rat.<sup>a)</sup>

Parameter	Compound	Base	$1 \times 10^{-6}$	$1 \times 10^{-5}$	$1 \times 10^{-4}$
Contractile force	<b>9g</b>	100 ± 2	115 ± 2	132 ± 6	179 ± 3
	Vesnarinone	100 ± 5	104 ± 1	126 ± 2	151 ± 1
Frequency rate	<b>6d</b>	100 ± 1	100 ± 4	110 ± 1	118 ± 5
	Vesnarinone	100 ± 5	105 ± 4	112 ± 4	121 ± 5

<sup>a)</sup> The pharmacological effect of each concentration (mol/L) of compound along with standard was articulated by the disparity between the force of retrenchment and frequency earlier than and after its inclusion to the bathing fluid, and were shown as a percentage difference in contraction and frequency in comparison with the controls. Results are presented as means ± SEM from six atria.

Bruker Avance-100 NMR spectrometer in DMSO-*d*<sub>6</sub> solution using TMS as an internal reference, respectively. MS spectra were recorded on an Agilent 1100 LC/MS.

The syntheses of compounds **1**, **2**, **3**, **4**, **6**, **7**, and **8** were performed in accordance with earlier reported procedures.

*General procedure for the synthesis of 4-(4-(1H-tetrazol-5-yl)-1H-pyrazol-1-yl)-6-morpholino-N-(substituted phenyl)-1,3,5-triazin-2-amine (9)*

A mixture of 1-(4-morpholino-6-((substituted phenyl)amino)-1,3,5-triazin-2-yl)-1H-pyrazole-4-carbonitrile (**8**) (0.1 mmol), sodium azide (0.2 mmol), and ammonium chloride (0.2 mmol) in 35 mL of DMF was heated at reflux temperature for 72 h. The reaction mixture was then poured into water and acidified with acid to make pH 5. The product was filtered and dried to afford the desired corresponding target derivatives in excellent yield.

*4-(4-(1H-Tetrazol-5-yl)-1H-pyrazol-1-yl)-N-(4-chlorophenyl)-6-morpholino-1,3,5-triazin-2-amine (9a)*

Yield: 76%; mp: 258–259°C; MW: 425.84; FT-IR ( $\nu_{\max}$ ; cm<sup>-1</sup> KBr): 3432 (N–H), 3064 (Ar C–H), 1628 (C=C), 1628 (C=N tetrazole), 1589 (C=N triazine), 1578 (–N=N–), 1082, 786 (C–Cl) cm<sup>-1</sup>; <sup>1</sup>H NMR (400 MHz, DMSO, TMS)  $\delta$  ppm: 9.82 (s, 1H, tetrazole), 8.94 (d, 1H, *J* = 1.6 Hz, pyrazole), 8.16 (d, 1H, *J* = 1.5 Hz, pyrazole), 7.73–7.41 (m, 4H, ArH), 3.74–3.65 (m, 8H, morpholine), 3.94 (s, 1H, N–H); <sup>13</sup>C NMR (100 MHz, CDCl<sub>3</sub>)  $\delta$  ppm: 179.4, 177.5, 167.3, 163.2, 137.6, 137.1, 129.8, 129.2, 127.7, 122.1, 102.4, 66.3, 48.7; Mass: 426.85 [M+1]; Elemental analysis for C<sub>17</sub>H<sub>16</sub>ClN<sub>11</sub>O: Calculated: C, 47.95; H, 3.79; N, 36.18; Found: C, 47.96; H, 3.81; N, 36.17.

*4-(4-(1H-Tetrazol-5-yl)-1H-pyrazol-1-yl)-N-(3-chlorophenyl)-6-morpholino-1,3,5-triazin-2-amine (9b)*

Yield: 72%; mp: 263–264°C; MW: 425.84; FT-IR ( $\nu_{\max}$ ; cm<sup>-1</sup> KBr): 3434 (N–H), 3062 (Ar C–H), 1625 (C=C), 1629 (C=N tetrazole), 1586 (C=N triazine), 1572 (–N=N–), 1086, 784 (C–Cl) cm<sup>-1</sup>; <sup>1</sup>H NMR (400 MHz, DMSO, TMS)  $\delta$  ppm: 9.86 (s, 1H, tetrazole), 8.93 (d, 1H, *J* = 1.6 Hz, pyrazole), 8.18 (d, 1H, *J* = 1.5 Hz, pyrazole), 7.78 (d, 1H, *J* = 8.1 Hz, Ar–H), 7.56 (t, 1H, *J* = 7.4 Hz, Ar–H), 7.34 (d, 1H, *J* = 8.2 Hz, Ar–H), 7.25 (d, 1H, *J* = 7.8 Hz, Ar–H), 3.74–3.67 (m, 8H, morpholine), 3.96 (s, 1H, N–H); <sup>13</sup>C NMR (100 MHz, CDCl<sub>3</sub>)  $\delta$  ppm: 179.2, 177.6, 167.3, 163.7, 143.9, 137.6, 135.2, 130.9, 129.3, 122.3, 116.7, 115.9, 102.4, 66.4, 48.9; Mass:

426.83 [M+1]; Elemental analysis for C<sub>17</sub>H<sub>16</sub>ClN<sub>11</sub>O: Calculated: C, 47.95; H, 3.79; N, 36.18; Found: C, 47.94; H, 3.80; N, 36.18.

*4-(4-(1H-Tetrazol-5-yl)-1H-pyrazol-1-yl)-N-(2-chlorophenyl)-6-morpholino-1,3,5-triazin-2-amine (9c)*

Yield: 76%; mp: 261–262°C; MW: 425.84; FT-IR ( $\nu_{\max}$ ; cm<sup>-1</sup> KBr): 3431 (N–H), 3065 (Ar C–H), 1628 (C=C), 1632 (C=N tetrazole), 1584 (C=N triazine), 1578 (–N=N–), 1089, 786 (C–Cl) cm<sup>-1</sup>; <sup>1</sup>H NMR (400 MHz, DMSO, TMS)  $\delta$  ppm: 9.85 (s, 1H, tetrazole), 8.94 (d, 1H, *J* = 1.8 Hz, pyrazole), 8.16 (d, 1H, *J* = 1.5 Hz, pyrazole), 7.76 (d, 1H, *J* = 7.5 Hz, Ar–H), 7.45 (t, 1H, *J* = 7.2 Hz, Ar–H), 7.31 (d, 1H, *J* = 7.3 Hz, Ar–H), 7.18 (d, 1H, *J* = 7.1 Hz, Ar–H), 3.74–3.68 (m, 8H, morpholine), 3.98 (s, 1H, N–H); <sup>13</sup>C NMR (100 MHz, CDCl<sub>3</sub>)  $\delta$  ppm: 179.2, 177.6, 167.3, 163.6, 137.8, 136.4, 130.8, 129.2, 127.6, 125.5, 122.9, 122.1, 102.3, 66.4, 48.7; Mass: 426.85 [M+1]; Elemental analysis for C<sub>17</sub>H<sub>16</sub>ClN<sub>11</sub>O: Calculated: C, 47.95; H, 3.79; N, 36.18; Found: C, 47.96; H, 3.79; N, 36.19.

*4-(4-(1H-Tetrazol-5-yl)-1H-pyrazol-1-yl)-N-(4-fluorophenyl)-6-morpholino-1,3,5-triazin-2-amine (9d)*

Yield: 79%; mp: 238–239°C; MW: 409.38; FT-IR ( $\nu_{\max}$ ; cm<sup>-1</sup> KBr): 3436 (N–H), 3057 (Ar C–H), 1623 (C=C), 1627 (C=N tetrazole), 1586 (C=N triazine), 1571 (–N=N–), 1159 (C–F) 1092 cm<sup>-1</sup>; <sup>1</sup>H NMR (400 MHz, DMSO, TMS)  $\delta$  ppm: 9.87 (s, 1H, tetrazole), 8.93 (d, 1H, *J* = 1.8 Hz, pyrazole), 8.17 (d, 1H, *J* = 1.5 Hz, pyrazole), 7.42–7.31 (m, 4H, Ar–H), 3.74–3.67 (m, 8H, morpholine), 3.97 (s, 1H, N–H); <sup>13</sup>C NMR (100 MHz, CDCl<sub>3</sub>)  $\delta$  ppm: 179.2, 177.6, 167.3, 163.7, 157.4, 137.7, 134.5, 129.3, 120.8, 116.3, 102.3, 66.3, 48.7; Mass: 410.39 [M+1]; Elemental analysis for C<sub>17</sub>H<sub>16</sub>FN<sub>11</sub>O: Calculated: C, 49.88; H, 3.94; N, 37.64; Found: C, 49.89; H, 3.94; N, 37.65.

*4-(4-(1H-Tetrazol-5-yl)-1H-pyrazol-1-yl)-N-(3-fluorophenyl)-6-morpholino-1,3,5-triazin-2-amine (9e)*

Yield: 74%; mp: 243–244°C; MW: 409.38; FT-IR ( $\nu_{\max}$ ; cm<sup>-1</sup> KBr): 3431 (N–H), 3058 (Ar C–H), 1627 (C=C), 1621 (C=N tetrazole), 1589 (C=N triazine), 1578 (–N=N–), 1162 (C–F) 1098 cm<sup>-1</sup>; <sup>1</sup>H NMR (400 MHz, DMSO, TMS)  $\delta$  ppm: 9.89 (s, 1H, tetrazole), 8.91 (d, 1H, *J* = 1.6 Hz, pyrazole), 8.17 (d, 1H, *J* = 1.5 Hz, pyrazole), 7.72 (d, 1H, *J* = 8.4 Hz, Ar–H), 7.52 (t, 1H, *J* = 7.3 Hz, Ar–H), 7.29 (d, 1H, *J* = 7.1 Hz, Ar–H), 6.98 (d, 1H, *J* = 5.4 Hz, Ar–H), 3.74–3.68 (m, 8H, morpholine), 3.97

(s, 1H, N–H);  $^{13}\text{C}$  NMR (100 MHz,  $\text{CDCl}_3$ )  $\delta$  ppm: 179.2, 177.6, 167.6, 163.8, 163.5, 144.2, 137.8, 131.2, 129.3, 113.4, 110.7, 104.9, 102.4, 66.4, 48.7; Mass: 410.41 [M+1]; Elemental analysis for  $\text{C}_{17}\text{H}_{16}\text{FN}_{11}\text{O}$ : Calculated: C, 49.88; H, 3.94; N, 37.64; Found: C, 49.89; H, 3.95; N, 37.65.

**4-(4-(1H-Tetrazol-5-yl)-1H-pyrazol-1-yl)-N-(2-fluorophenyl)-6-morpholino-1,3,5-triazin-2-amine (9f)**

Yield: 69%; mp: 247–248°C; MW: 409.38; FT-IR ( $\nu_{\text{max}}$ ;  $\text{cm}^{-1}$  KBr): 3435 (N–H), 3056 (Ar C–H), 1624 (C=C), 1625 (C=N tetrazole), 1584 (C=N triazine), 1579 (–N=N–), 1156 (C–F)  $1094\text{ cm}^{-1}$ ;  $^1\text{H}$  NMR (400 MHz, DMSO, TMS)  $\delta$  ppm: 9.91 (s, 1H, tetrazole), 8.87 (d, 1H,  $J=1.6$  Hz, pyrazole), 8.21 (t, 1H,  $J=7.6$  Hz, Ar–H), 8.16 (d, 1H,  $J=1.5$  Hz, pyrazole), 7.26 (t, 1H,  $J=7.2$  Hz, Ar–H), 7.04 (d, 1H,  $J=6.9$  Hz, Ar–H), 7.02 (d, 1H,  $J=6.8$  Hz, Ar–H), 3.74–3.67 (m, 8H, morpholine), 3.96 (s, 1H, N–H);  $^{13}\text{C}$  NMR (100 MHz,  $\text{CDCl}_3$ )  $\delta$  ppm: 179.2, 177.6, 167.2, 163.6, 154.8, 137.8, 129.3, 128.2, 125.1, 123.8, 123.2, 116.4, 102.4, 66.4, 48.7; Mass: 410.36 [M+1]; Elemental analysis for  $\text{C}_{17}\text{H}_{16}\text{FN}_{11}\text{O}$ : Calculated: C, 49.88; H, 3.94; N, 37.64; Found: C, 49.90; H, 3.94; N, 37.64.

**4-(4-(1H-Tetrazol-5-yl)-1H-pyrazol-1-yl)-6-morpholino-N-(4-nitrophenyl)-1,3,5-triazin-2-amine (9g)**

Yield: 82%; mp: 258–259°C; MW: 436.39; FT-IR ( $\nu_{\text{max}}$ ;  $\text{cm}^{-1}$  KBr): 3432 (N–H), 3059 (Ar C–H), 1627 (C=C), 1628 (C=N tetrazole), 1587 (C=N triazine), 1582 (–N=N–), 1528 ( $\text{NO}_2$  str), 1098,  $712\text{ cm}^{-1}$ ;  $^1\text{H}$  NMR (400 MHz, DMSO, TMS)  $\delta$  ppm: 9.92 (s, 1H, tetrazole), 8.89 (d, 1H,  $J=1.6$  Hz, pyrazole), 8.17 (d, 1H,  $J=1.5$  Hz, pyrazole), 8.12–7.36 (m, 4H, Ar–H), 3.74–3.66 (m, 8H, morpholine), 3.97 (s, 1H, N–H);  $^{13}\text{C}$  NMR (100 MHz,  $\text{CDCl}_3$ )  $\delta$  ppm: 179.2, 177.4, 167.3, 163.6, 145.2, 137.9, 137.7, 129.2, 124.7, 119.2, 102.3, 66.3, 48.7; Mass: 437.40 [M+1]; Elemental analysis for  $\text{C}_{17}\text{H}_{16}\text{N}_{12}\text{O}_3$ : Calculated: C, 46.79; H, 3.70; N, 38.52; Found: C, 46.80; H, 3.69; N, 38.52.

**4-(4-(1H-Tetrazol-5-yl)-1H-pyrazol-1-yl)-6-morpholino-N-(3-nitrophenyl)-1,3,5-triazin-2-amine (9h)**

Yield: 69%; mp: 264–265°C; MW: 436.39; FT-IR ( $\nu_{\text{max}}$ ;  $\text{cm}^{-1}$  KBr): 3435 (N–H), 3061 (Ar C–H), 1624 (C=C), 1622 (C=N tetrazole), 1589 (C=N triazine), 1584 (–N=N–), 1529 ( $\text{NO}_2$  str), 1094,  $718\text{ cm}^{-1}$ ;  $^1\text{H}$  NMR (400 MHz, DMSO, TMS)  $\delta$  ppm: 9.94 (s, 1H, tetrazole), 8.86 (d, 1H,  $J=1.6$  Hz, pyrazole), 8.18 (d, 1H,  $J=1.5$  Hz, pyrazole), 8.02 (d, 1H,  $J=3.4$  Hz, Ar–H), 7.62 (d, 1H,  $J=8.3$  Hz, Ar–H), 7.56 (d, 1H,  $J=7.4$  Hz, Ar–H), 7.45 (t, 1H,  $J=7.1$  Hz, Ar–H), 3.74–3.67 (m, 8H, morpholine), 3.96 (s, 1H, N–H);  $^{13}\text{C}$  NMR (100 MHz,  $\text{CDCl}_3$ )  $\delta$  ppm: 179.2, 177.5, 167.3, 163.5, 148.8, 143.4, 137.6, 130.4, 129.2, 123.9, 113.8, 109.2, 102.3, 66.4, 48.7; Mass: 437.38 [M+1]; Elemental analysis for  $\text{C}_{17}\text{H}_{16}\text{N}_{12}\text{O}_3$ : Calculated: C, 46.79; H, 3.70; N, 38.52; Found: C, 46.78; H, 3.70; N, 38.53.

**4-(4-(1H-Tetrazol-5-yl)-1H-pyrazol-1-yl)-6-morpholino-N-(2-nitrophenyl)-1,3,5-triazin-2-amine (9i)**

Yield: 65%; mp: 267–268°C; MW: 436.39; FT-IR ( $\nu_{\text{max}}$ ;  $\text{cm}^{-1}$  KBr): 3432 (N–H), 3064 (Ar C–H), 1621 (C=C), 1627 (C=N

tetrazole), 1583 (C=N triazine), 1589 (–N=N–), 1525 ( $\text{NO}_2$  str), 1091,  $715\text{ cm}^{-1}$ ;  $^1\text{H}$  NMR (400 MHz, DMSO, TMS)  $\delta$  ppm: 9.95 (s, 1H, tetrazole), 8.84 (d, 1H,  $J=1.6$  Hz, pyrazole), 8.14 (d, 1H,  $J=1.5$  Hz, pyrazole), 8.08 (d, 1H,  $J=7.8$  Hz, Ar–H), 7.65 (d, 1H,  $J=7.5$  Hz, Ar–H), 7.64 (t, 1H,  $J=7.3$  Hz, Ar–H), 7.41 (t, 1H,  $J=7.4$  Hz, Ar–H), 3.74–3.68 (m, 8H, morpholine), 3.95 (s, 1H, N–H);  $^{13}\text{C}$  NMR (100 MHz,  $\text{CDCl}_3$ )  $\delta$  ppm: 179.2, 177.5, 167.3, 163.4, 144.7, 137.8, 137.2, 129.3, 129.1, 125.8, 119.7, 110.5, 102.3, 66.4, 48.8; Mass: 437.42 [M+1]; Elemental analysis for  $\text{C}_{17}\text{H}_{16}\text{N}_{12}\text{O}_3$ : Calculated: C, 46.79; H, 3.70; N, 38.52; Found: C, 46.80; H, 3.71; N, 38.52.

**4-(4-(1H-Tetrazol-5-yl)-1H-pyrazol-1-yl)-6-morpholino-N-(p-tolyl)-1,3,5-triazin-2-amine (9j)**

Yield: 84%; mp: 243–244°C; MW: 405.42; FT-IR ( $\nu_{\text{max}}$ ;  $\text{cm}^{-1}$  KBr): 3434 (N–H), 3052 (Ar C–H), 2981 ( $\text{CH}_3$  str), 1625 (C=C), 1629 (C=N tetrazole), 1581 (C=N triazine), 1586 (–N=N–), 1093,  $712\text{ cm}^{-1}$ ;  $^1\text{H}$  NMR (400 MHz, DMSO, TMS)  $\delta$  ppm: 9.92 (s, 1H, tetrazole), 8.86 (d, 1H,  $J=1.6$  Hz, pyrazole), 8.16 (d, 1H,  $J=1.5$  Hz, pyrazole), 7.24–7.04 (m, 4H, Ar–H), 3.74–3.67 (m, 8H, morpholine), 3.97 (s, 1H, N–H), 2.34 (s, 3H,  $\text{CH}_3$ );  $^{13}\text{C}$  NMR (100 MHz,  $\text{CDCl}_3$ )  $\delta$  ppm: 179.2, 177.6, 167.3, 163.6, 137.6, 135.8, 131.2, 129.9, 129.3, 120.3, 102.4, 66.4, 48.8, 21.2; Mass: 406.41 [M+1]; Elemental analysis for  $\text{C}_{18}\text{H}_{19}\text{N}_{11}\text{O}$ : Calculated: C, 53.33; H, 4.72; N, 38.00; Found: C, 53.35; H, 4.71; N, 38.02.

**4-(4-(1H-Tetrazol-5-yl)-1H-pyrazol-1-yl)-6-morpholino-N-(m-tolyl)-1,3,5-triazin-2-amine (9k)**

Yield: 65%; mp: 250–251°C; MW: 405.42; FT-IR ( $\nu_{\text{max}}$ ;  $\text{cm}^{-1}$  KBr): 3438 (N–H), 3056 (Ar C–H), 2983 ( $\text{CH}_3$  str), 1627 (C=C), 1636 (C=N tetrazole), 1586 (C=N triazine), 1578 (–N=N–), 1091,  $719\text{ cm}^{-1}$ ;  $^1\text{H}$  NMR (400 MHz, DMSO, TMS)  $\delta$  ppm: 9.95 (s, 1H, tetrazole), 8.87 (d, 1H,  $J=1.6$  Hz, pyrazole), 8.18 (d, 1H,  $J=1.5$  Hz, pyrazole), 7.52 (d, 1H,  $J=8.2$  Hz, Ar–H), 7.44 (d, 1H,  $J=7.2$  Hz, Ar–H), 7.18 (d, 1H,  $J=6.4$  Hz, Ar–H), 6.89 (d, 1H,  $J=5.2$  Hz, Ar–H), 3.74–3.68 (m, 8H, morpholine), 3.98 (s, 1H, N–H), 2.35 (s, 3H,  $\text{CH}_3$ );  $^{13}\text{C}$  NMR (100 MHz,  $\text{CDCl}_3$ )  $\delta$  ppm: 179.2, 177.6, 167.3, 163.7, 142.3, 139.2, 137.8, 129.4, 129.1, 121.2, 119.4, 114.8, 102.4, 21.3, 66.4, 48.8, 21.3; Mass: 406.43 [M+1]; Elemental analysis for  $\text{C}_{18}\text{H}_{19}\text{N}_{11}\text{O}$ : Calculated: C, 53.33; H, 4.72; N, 38.00; Found: C, 53.32; H, 4.72; N, 38.01.

**4-(4-(1H-Tetrazol-5-yl)-1H-pyrazol-1-yl)-6-morpholino-N-(o-tolyl)-1,3,5-triazin-2-amine (9l)**

Yield: 62%; mp: 254–255°C; MW: 405.42; FT-IR ( $\nu_{\text{max}}$ ;  $\text{cm}^{-1}$  KBr): 3432 (N–H), 3054 (Ar C–H), 2981 ( $\text{CH}_3$  str), 1629 (C=C), 1639 (C=N tetrazole), 1585 (C=N triazine), 1572 (–N=N–), 1095,  $712\text{ cm}^{-1}$ ;  $^1\text{H}$  NMR (400 MHz, DMSO, TMS)  $\delta$  ppm: 9.91 (s, 1H, tetrazole), 8.85 (d, 1H,  $J=1.6$  Hz, pyrazole), 8.17 (d, 1H,  $J=1.5$  Hz, pyrazole), 7.15 (d, 1H,  $J=2.4$  Hz, Ar–H), 7.02 (t, 1H,  $J=1.8$  Hz, Ar–H), 6.76 (t, 1H,  $J=1.9$  Hz, Ar–H), 6.48 (d, 1H,  $J=1.3$  Hz, Ar–H), 3.74–3.68 (m, 8H, morpholine), 3.97 (s, 1H, N–H), 2.18 (s, 3H,  $\text{CH}_3$ );  $^{13}\text{C}$  NMR (100 MHz,  $\text{CDCl}_3$ )  $\delta$  ppm: 179.2, 177.6, 167.2, 163.7, 142.4, 137.7, 131.4, 129.2, 128.9, 126.4, 123.8, 123.7, 102.3, 66.4, 48.7, 17.6; Mass: 406.41

[M+1]; Elemental analysis for  $C_{18}H_{19}N_{11}O$ : Calculated: C, 53.33; H, 4.72; N, 38.00; Found: C, 53.33; H, 4.73; N, 38.02.

**4-(4-(1H-Tetrazol-5-yl)-1H-pyrazol-1-yl)-N-(4-methoxyphenyl)-6-morpholino-1,3,5-triazin-2-amine (9m)**

Yield: 83%; mp: 271–272°C; MW: 421.42; FT-IR ( $\nu_{\max}$ ;  $cm^{-1}$  KBr): 3437 (N–H), 3052 (Ar C–H), 2924 (OCH<sub>3</sub> str), 1636 (C=C), 1642 (C=N tetrazole), 1589 (C=N triazine), 1576 (–N=N–), 1096, 713  $cm^{-1}$ ; <sup>1</sup>H NMR (400 MHz, DMSO, TMS)  $\delta$  ppm: 9.95 (s, 1H, tetrazole), 8.89 (d, 1H,  $J$  = 1.6 Hz, pyrazole), 8.14 (d, 1H,  $J$  = 1.5 Hz, pyrazole), 7.26–6.62 (m, 4H, Ar–H), 3.72–3.67 (m, 8H, morpholine), 3.95 (s, 1H, N–H), 3.84 (s, 3H, OCH<sub>3</sub>); <sup>13</sup>C NMR (100 MHz, CDCl<sub>3</sub>)  $\delta$  ppm: 179.2, 177.5, 167.3, 163.6, 153.4, 137.7, 131.3, 129.3, 121.8, 115.2, 102.4, 66.5, 55.9, 48.8; Mass: 422.44 [M+1]; Elemental analysis for  $C_{18}H_{19}N_{11}O_2$ : Calculated: C, 51.30; H, 4.54; N, 36.56; Found: C, 51.31; H, 4.54; N, 36.54.

**4-(4-(1H-Tetrazol-5-yl)-1H-pyrazol-1-yl)-N-(3-methoxyphenyl)-6-morpholino-1,3,5-triazin-2-amine (9n)**

Yield: 74%; mp: 278–279°C; MW: 421.42; FT-IR ( $\nu_{\max}$ ;  $cm^{-1}$  KBr): 3431 (N–H), 3059 (Ar C–H), 2928 (OCH<sub>3</sub> str), 1631 (C=C), 1649 (C=N tetrazole), 1586 (C=N triazine), 1572 (–N=N–), 1098, 712  $cm^{-1}$ ; <sup>1</sup>H NMR (400 MHz, DMSO, TMS)  $\delta$  ppm: 9.93 (s, 1H, tetrazole), 8.87 (d, 1H,  $J$  = 1.6 Hz, pyrazole), 8.18 (d, 1H,  $J$  = 1.5 Hz, pyrazole), 7.21 (d, 1H,  $J$  = 5.8 Hz, Ar–H), 7.08 (t, 1H,  $J$  = 5.3 Hz, Ar–H), 6.38 (d, 1H,  $J$  = 4.3 Hz, Ar–H), 6.18 (d, 1H,  $J$  = 4.1 Hz, Ar–H), 3.73–3.69 (m, 8H, morpholine), 3.96 (s, 1H, N–H), 3.82 (s, 3H, OCH<sub>3</sub>); <sup>13</sup>C NMR (100 MHz, CDCl<sub>3</sub>)  $\delta$  ppm: 179.2, 177.5, 167.3, 163.6, 161.4, 143.4, 137.8, 130.5, 129.2, 110.8, 110.2, 102.4, 99.6, 66.4, 55.9, 48.9; Mass: 422.40 [M+1]; Elemental analysis for  $C_{18}H_{19}N_{11}O_2$ : Calculated: C, 51.30; H, 4.54; N, 36.56; Found: C, 51.33; H, 4.55; N, 36.55.

**4-(4-(1H-Tetrazol-5-yl)-1H-pyrazol-1-yl)-N-(2-methoxyphenyl)-6-morpholino-1,3,5-triazin-2-amine (9o)**

Yield: 68%; mp: 275–276°C; MW: 421.42; FT-IR ( $\nu_{\max}$ ;  $cm^{-1}$  KBr): 3437 (N–H), 3064 (Ar C–H), 2924 (OCH<sub>3</sub> str), 1634 (C=C), 1642 (C=N tetrazole), 1586 (C=N triazine), 1574 (–N=N–), 1095, 713  $cm^{-1}$ ; <sup>1</sup>H NMR (400 MHz, DMSO, TMS)  $\delta$  ppm: 9.97 (s, 1H, tetrazole), 8.89 (d, 1H,  $J$  = 1.6 Hz, pyrazole), 8.18 (d, 1H,  $J$  = 1.5 Hz, pyrazole), 6.89 (d, 1H,  $J$  = 4.8 Hz, Ar–H), 6.78 (t, 1H,  $J$  = 4.5 Hz, Ar–H), 6.68 (d, 1H,  $J$  = 4.2 Hz, Ar–H), 6.48 (d, 1H,  $J$  = 3.2 Hz, Ar–H), 3.74–3.67 (m, 8H, morpholine), 3.97 (s, 1H, N–H), 3.84 (s, 3H, OCH<sub>3</sub>); <sup>13</sup>C NMR (100 MHz, CDCl<sub>3</sub>)  $\delta$  ppm: 179.2, 177.5, 167.2, 163.5, 147.4, 137.6, 132.7, 129.2, 122.7, 121.9, 113.4, 112.1, 102.4, 66.4, 55.9, 48.8; Mass: 422.43 [M+1]; Elemental analysis for  $C_{18}H_{19}N_{11}O_2$ : Calculated: C, 51.30; H, 4.54; N, 36.56; Found: C, 51.32; H, 4.54; N, 36.56.

## Pharmacological activity

### Animals, drugs, chemicals, and instruments

The adult male Wistar rats weighing 250–350 g were obtained from the animal house of the institute and kept in optimum conditions (temperature:  $23 \pm 2^\circ C$ ; light–dark cycle: 7 am to

7 pm). In order to prevent any stress in the experimental animal, they had the free access to a standard laboratory diet and water. To obtain a trial fragments, the rats were pre-treated intraperitoneally with reserpine (5 mg/kg body weight) to prevent any interference of endogenous CAs on the results [10]. In every experimentation, the rats were made unconscious with intraperitoneal injection of thiopental (a barbiturate derivative) in 80 mg/kg. Under the influence of anesthesia, midline thoracotomy was performed and the heart was rapidly removed. The isolated heart without delay was rapidly transferred into dissection plate packed with oxygenated Krebs–Henseleit solution. The required enzymes were obtained from BPS BioScience, Inc.

### Assessment of PDE3A and PDE3B inhibitory activities

Briefly, at room temperature, the desired enzymatic reaction was performed for 60 min in 50  $\mu L$  mixture containing IMAP reaction buffer, 100 nM FAM-cAMP, 1 ng PDE3A or PDE3B, and the synthesized analogs. The reactions were performed in the presence of binding reagent made in 1:600 dilution in a reagent binding buffer containing 85% Binding Buffer A and 15% Binding Buffer B at room temperature for 60 min. The assays were executed twice at each concentration and the resultant fluorescence intensity, determined by microplate reader, is converted into fluorescence polarization. The highest value of fluorescence polarization ( $FP_t$ ) in each data set was assumed as 100% activity, in the absence of PDE3, it was assumed to be 0% activity. The percentage of activity in the presence of the compound was calculated with the help of the following equation: %binding =  $(FP - FP_b)/(FP_t - FP_b) \times 100$ , where  $FP$  is the fluorescence polarization (with compound),  $FP_b$  is the fluorescent polarization (absence of PDE3), and  $FP_t$  corresponds to the highest fluorescent polarization in each data set. The  $IC_{50}$  values were determined accordingly from the percent activity of the enzymes at different concentrations of synthetic inhibitors.

### Evaluation of inotropic and chronotropic activities

The whole atrium was detached from the ventricle and mounted vertically in a 50 mL organ-bath containing Krebs–Henseleit solution which was regularly gassed by 95% O<sub>2</sub> and 5% CO<sub>2</sub> in 35–37°C with a pH of 7.35–7.45. Whereas, the bathing solution was prepared (in mM) using NaCl 118, KCl 4.5, CaCl<sub>2</sub> 1.36, MgSO<sub>4</sub> 1.21, NaH<sub>2</sub>PO<sub>4</sub> 1.22, NaHCO<sub>3</sub> 25, and glucose 11. The resting tension was attuned to about 0.5 g in the whole atria and the initial equilibration period was achieved for each preparation. To verify the blockage of endogeneous CAs, the atria that did not show any positive inotropic effect induced by tyramine (1.5  $\mu M$ ) were selected for further experimentation. The test compounds were added in the graded dose of 1–100  $\mu M$  and the responses of each concentration were documented up to the maximum limit. The force transducer (type E. Zimmermann, Leipzig, Berlin) connected to PowerLab 8/30 (model 870) was utilized to record developed tension.

## Molecular docking studies

The three dimensional (3D) crystal structure of catalytic domain of human phosphodiesterase 3b in complex with a dihydropyridazine inhibitor (1SO2) was retrieved from the protein data bank (PDB) (Source: [www.rcsb.org/pdb](http://www.rcsb.org/pdb)). The native autoinducer and all water molecules were removed. The CHARMM force field (FF) was used to add atom types and hydrogens in the proteins. 3D structures of all synthesized compounds were constructed and energy minimized using the Discovery Studio 2.5/Builder module. Docking studies were performed using the CDOCKER module of Discovery Studio 2.5. CDOCKER is a grid-based molecular docking method where the receptor is held rigid while the ligands are allowed to flex during the refinement. The CHARMM force field was used as an energy grid force field for docking and scoring function calculations. Random ligand conformations were generated from the initial structure through high temperature molecular dynamics, followed by random rotations which were further refined by grid-based (GRID 1) simulated annealing and a final grid-based minimization. Of the 10 best poses, one (conformation) having a highest docking score (-CDOCKER energy) was used for the binding energy calculations and further analysis. The higher negative value of CDOCKER energy represents more favorable binding of the complex. CDOCKER score (-CDOCKER Energy) includes internal ligand strain energy and receptor–ligand interaction energy, and is used to sort the different conformations of each input ligand.

The authors have declared no conflicts of interest.

## References

- [1] World Health Organization. Noncommunicable diseases. Fact sheet. Updated January 2015. Available from URL: <http://www.who.int/mediacentre/factsheets/fs355/en/>
- [2] WHO, The World Health Report, 2002: Reducing risks, promoting healthy life. Geneva: World Health Organization 2002.
- [3] M. Ezzati, A. D. Lopez, A. Rodgers, S. Vander Hoorn, C. J. L. Murray, *Lancet* **2002**, *360*, 1347–1360.
- [4] M. C. Scott, M. E. Winters, *Emerg. Med. Clin. North Am.* **2015**, *33*, 553–562.
- [5] S. Jain, B. Vaidyanathan, *Ann. Pediatr. Cardiol.* **2009**, *2*, 149–152.
- [6] M. Guazzi, *Circ. Heart Fail.* **2008**, *1*, 272–280.
- [7] K. Omori, J. Kotera, *Circ. Res.* **2007**, *100*, 309–327.
- [8] D. Ramos Martins, F. Pazini, V. de Medeiros Alves, S. Santana de Moura, L. Morais Lião, M. Torquato Quezado de Magalhães, M. Campos Valadares, C. Horta Andrade, R. Menegatti, M. Lavorenti Rocha, *Chem. Pharm. Bull.* **2013**, *61*, 524–531.
- [9] L. M. Duan, H. Y. Yu, Y. L. Li, C. J. Jia, *Bioorg. Med. Chem.* **2015**, *23*, 6111–6117.
- [10] B. Singh, H. R. Bhat, M. K. Kumawat, U. P. Singh, *Bioorg. Med. Chem. Lett.* **2014**, *24*, 3321–3325.
- [11] H. R. Bhat, U. P. Singh, P. Gahtori, S. K. Ghosh, K. Gogoi, A. Prakash, R. K. Singh, *Chem. Biol. Drug Des.* **2015**, *86*, 265–271.
- [12] B. Pogorelčnik, M. Janežič, I. Sosič, S. Gobec, T. Solmajer, A. Perdih, *Bioorg. Med. Chem.* **2015**, *23*, 4218–4229.
- [13] U. P. Singh, H. R. Bhat, P. Gahtori, *J. Mycol. Med.* **2012**, *22*, 134–141.
- [14] J. K. Srivastava, P. Dubey, S. Singh, H. R. Bhat, M. K. Kumawat, U. P. Singh, *RSC Adv.* **2015**, *5*, 14095–14102.
- [15] J. K. Srivastava, N. T. Awatade, H. R. Bhat, A. Kmit, K. Mendes, M. Ramos, M. D. Amaral, U. P. Singh, *RSC Adv.* **2015**, *5*, 88710–88718.
- [16] F. Carta, V. Garaj, A. Maresca, J. Wagner, B. S. Avvaru, A. H. Robbins, A. Scozzafava, R. McKenna, C. T. Supuran, *Bioorg. Med. Chem.* **2011**, *19*, 3105–3119.
- [17] V. Lozano, L. Aguado, B. Hoorelbeke, M. Renders, M. J. Camarasa, D. Schols, J. Balzarini, A. San-Félix, M. J. Pérez-Pérez, *J. Med. Chem.* **2011**, *54*, 5335–5348.
- [18] X. Y. Meng, H. X. Zhang, M. Mezei, M. Cui, *Curr. Comput. Aided Drug Des.* **2011**, *7*, 146–157.
- [19] C. J. LaBuda, P. N. Fuchs, *Alcohol* **2002**, *26*, 55–59.